Nanoscale

COMMUNICATION

View Article Online
View Journal | View Issue



Cite this: *Nanoscale*, 2016, **8**, 5815

Received 13th December 2015,
Accepted 18th February 2016

DOI: 10.1039/c5nr08866f

www.rsc.org/nanoscale

# A graphene-based affinity nanosensor for detection of low-charge and low-molecular-weight molecules†

Yibo Zhu,[a] Yufeng Hao,[a] Enoch A. Adogla,[b] Jing Yan,[b] Dachao Li,[c] Kexin Xu,[c] Qian Wang,[b] James Hone[a] and Qiao Lin*[a]

**This paper presents a graphene nanosensor for affinity-based detection of low-charge, low-molecular-weight molecules, using glucose as a representative. The sensor is capable of measuring glucose concentration in a practically relevant range of 2 μM to 25 mM, and can potentially be used in noninvasive glucose monitoring.**

Graphene is emerging as an attractive functional nanomaterial in sensors that allow highly sensitive detection of chemical and biological analytes.[1–3] In particular, field effect transistor (FET) sensors that use graphene as the conducting channel have been used in both gaseous and liquid media.[4,5] Analytes detectable by these sensors are typically highly charged or are strong electron donors or acceptors, which readily induce significant carrier doping in graphene for FET-based measurements. The development of graphene nanosensors to detect analytes of low charge and low molecular weight, however, still remains a challenge.[6,7]

Glucose, one of the uncharged, low-molecular-weight molecules, is of fundamental importance to people life health. Abnormal levels of glucose concentration in blood, if not properly monitored and corrected, can cause severe or even life-threatening complications to patients with diabetes or other related diseases. Graphene FET based enzymatic sensors have been reported to enable sensitive detection of glucose.[7,8] Unfortunately, due to the irreversible, consumptive nature of the enzyme-catalyzed electrochemical reactions of glucose, as well as the undesirable byproduct (*e.g.*, hydrogen peroxide) generated in the reactions of enzymes and glucose, these enzyme-based sensors would suffer from significant limitations in stability and accuracy when operating in physiological environments.[9]

In contrast, affinity sensing, based on non-reactive equilibrium binding of analyte with an affinity receptor, neither consumes the target analyte nor produces any byproduct, therefore can potentially be implanted for stable and accurate glucose monitoring.[9] Affinity glucose sensing has been implemented using optical, mechanical, and electrical methods on conventional or microscale platforms.[10–13] While demonstrating the potential of affinity glucose sensing, these methods typically require complex sensor structures (*e.g.*, moving mechanical components or physical barriers), and may not have sufficient sensitivity in human bodily fluids such as tears or saliva, in which glucose concentrations are one or two orders of magnitude lower than that in blood.[14–17] Affinity glucose sensing using functional nanomaterials is to date rather scarce. Boron-doped graphene quantum dots have been used for affinity glucose sensing, although its requirement of an additional optical measurement system is not amenable to miniaturization.[18] Boronic acid functionalized carbon nanotubes (CNTs) have also been used for glucose detection in deionized water. Nevertheless, these sensors relied on the contact among the randomly distributed, entangled nanotubes and may not be well suited to practical applications because of a lack of consistency and stability.[19] Furthermore, the underlying sensing mechanisms have not been clarified due to the difficulties in precise determination of the weak doping induced by the affinity binding in the semiconducting CNTs.

This paper presents an atomically thin, graphene-based sensor for affinity-based detection of glucose, an uncharged, low-molecular-weight molecule. This nanosensor employs a graphene FET in which graphene is functionalized with boronic acid for glucose recognition. In contrast to the multi-step chemical modification procedure that is required for enzyme based graphene glucose sensors, the functionalization in our sensor is enabled by a simple one-step method *via* the interaction of graphene with pyrene-terminated boronic acid. This method allows boronic acid to be closely attached to the graphene surface, thereby the binding of boronic acid with

[a]*Department of Mechanical Engineering, Columbia University, New York, NY 10027, USA. E-mail: qlin@columbia.edu*
[b]*Department of Chemistry and Biochemistry, University of South Carolina, Columbia, SC 29208, USA*
[c]*College of Precision Instrument and Opto-Electronic Engineering, Tianjin University, Tianjin, 300072, China*

† Electronic supplementary information (ESI) available: Further details on experiments, materials, fabrication, and data analysis. See DOI: 10.1039/c5nr08866f

glucose can significantly change the electrical properties of graphene, and enables sensitive detection of the glucose molecules. Moreover, the bipolar transfer characteristics of graphene, thanks to its vanishing bandgap and high mobility, exhibit significant and definitive shifts upon glucose-boronic acid binding. This shift can reflect affinity binding-induced charge transfer to graphene, or changes in the electrostatic potential in the immediate proximity of graphene, thereby allowing for insights into the underlying physicochemical mechanisms for affinity glucose recognition on the nanomaterial. For potential clinical applications, the coupling of graphene with boronic acid *via* stable chemical bonding eliminates the needs for mechanical movable structures or physical barriers that are commonly used in existing affinity glucose sensors.[11,20] Therefore, it simplifies the device design and potentially enables a consistent, rapidly responsive measurement for noninvasive glucose monitoring. For example, wearable glucose monitoring devices can be realized by integrating these sensors with contact lens to detect the glucose concentration in tears.

The affinity glucose nanosensor was configured as a solution-gated graphene FET (Fig. 1a). The graphene, serving as the conducting channel (Fig. 1b), was functionalized with pyrene-1-boronic acid (PBA) *via* π–π stacking interactions (Fig. 1c). The device was fabricated using micro and nanofabrication techniques (see details in ESI†). A polydimethylsiloxane (PDMS)-based open well (~20 μL) was bonded to the substrate; and glucose solution was placed into the well. An Ag/AgCl reference electrode, mounted on a three-axis positioner, was inserted into the solution to serve as the gate electrode. An electrical double layer (EDL) formed at the interface of the graphene and solution served as the gate capacitor. Binding of glucose and the boronic acid formed a glucose-boronate ester complex (Fig. 1d), inducing changes in the electric conductance of the graphene, which was measured to determine the glucose concentration.

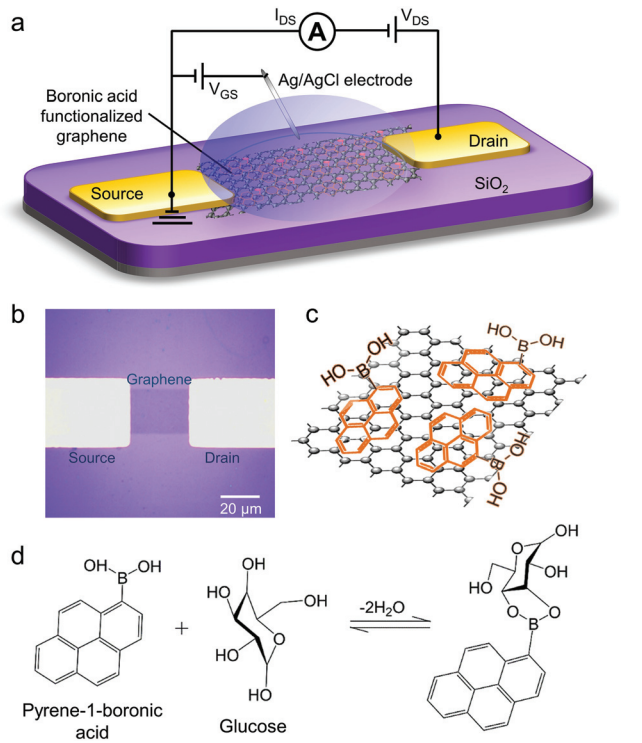


**Fig. 1** (a) Schematic of the nanosensor configured as a solution-gated graphene field effect transistor. An Ag/AgCl electrode inserted into the solution served as the gate electrode, while the electrical double layer at the solution-graphene interface served as the gate capacitor. (b) Micrograph of a fabricated device. The graphene conducting channel connected the source and drain electrodes. (c) Coupling of boronic acid and graphene *via* π–π stacking interactions between the pyrene group and graphene. (d) Formation of a glucose-boronate ester at a physiological pH of 7.4.

In a solution-gated FET, the capacitance of the double layer can be influenced by the solution composition. Prior to any chemical functionalization of the graphene, we first examined the fluctuations of the EDL capacitance that can possibly be attributed to changes in the glucose concentration. Glucose was dissolved in phosphate buffered solution (pH 7.4) to obtain desired concentrations (2 μM to 25 mM). The same solutions were used in all of the subsequent experiments. Without any chemical functionalization of graphene, the transfer characteristics (source–drain current $I_{DS}$ as a function of gate voltage $V_{GS}$) measured at the different glucose concentrations were almost indistinguishable (Fig. 2a). This suggested that glucose, at the selected concentration range, did not either interact with graphene or vary the capacitance of the double layer, in agreement with previous related studies.[19,21]

This device was then immersed in PBA solution for 4 hours at room temperature, followed by sequentially rinsing in acetonitrile, isopropanol and deionized water to remove free PBA. In prior to the chemical functionalization, in the Raman spectrum (Fig. 2b) of the graphene at the channel region, the ratio of the intensity of the 2D band to the G band ($I_{2D}/I_G$) was 2.5, and the full width at half maximum (FWHM) of the 2D band was ~27 from Lorentz fitting, both of which were further evidence of monolayer graphene[22,23] in addition to the color contrast observed under microscope (Fig. 1b). The Raman spectrum of the PBA solution-rinsed graphene exhibited signature peaks of BOH bending (1286 $cm^{-1}$), B–O stretching (1378 $cm^{-1}$), and G-band splitting (1574, 1595, 1613 $cm^{-1}$) due to the graphene-pyrene π–π stacking interaction.[24–27] Also, the 2D band shifted to a higher wavenumber (from 2685 to 2692 $cm^{-1}$), which was considered as a result of chemical doping.[28] The measured transfer characteristics (Fig. 2a) also verified the chemically induced p-type doping, represented by the increase of the neutral point voltage $V_{NP}$ (the gate voltage at which $I_{DS}$ attains its minimum) from 0.33 V to 0.575 V. These observed characteristics of the boronic acid as well as the graphene–pyrene interaction confirmed that the PBA molecules were successfully immobilized on the graphene. Further details on characterization of graphene and chemical functionalization can be found in ESI.†

After functionalization, it was confirmed that replenishment of sample solution to the nanosensor did not interrupt the pyrene–graphene coupling (Fig. S3†). Then the sensor was

 

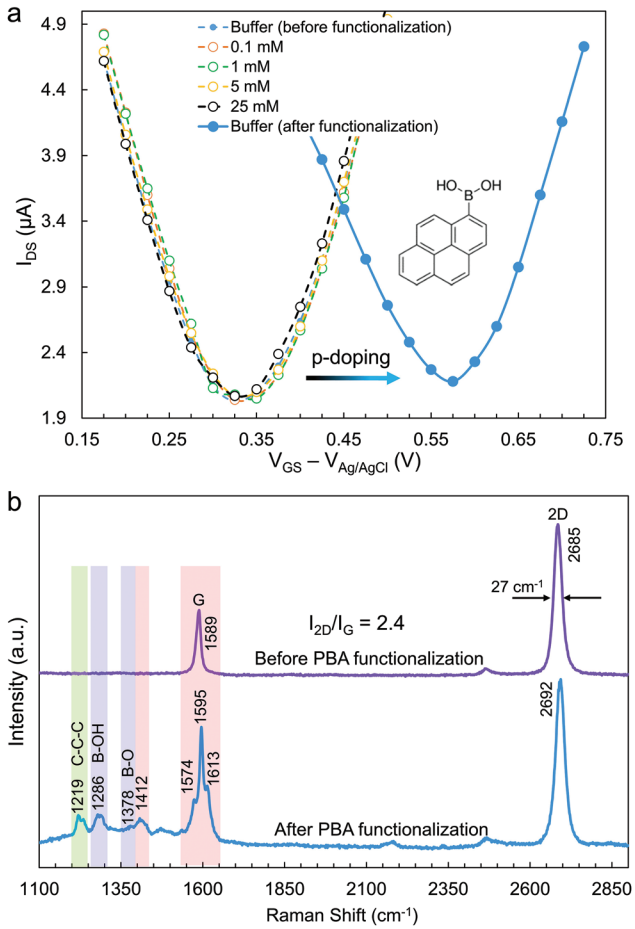


Fig. 2 (a) Transfer characteristics of the pristine graphene and the PBA-functionalized graphene. Dashed lines: transfer characteristics of the pristine graphene exposed to glucose solutions (0.1 mM to 25 mM). Solid lines: transfer characteristics after rinsing with PBA solution. $V_{NP}$ shifted from 0.33 V to 0.575 V. Legend: Glucose concentrations. (b) Raman spectra of the graphene before and after exposure to PBA solution. Signature peaks of the boronic acid and the graphene–pyrene interaction were observed after immersing in PBA solution.

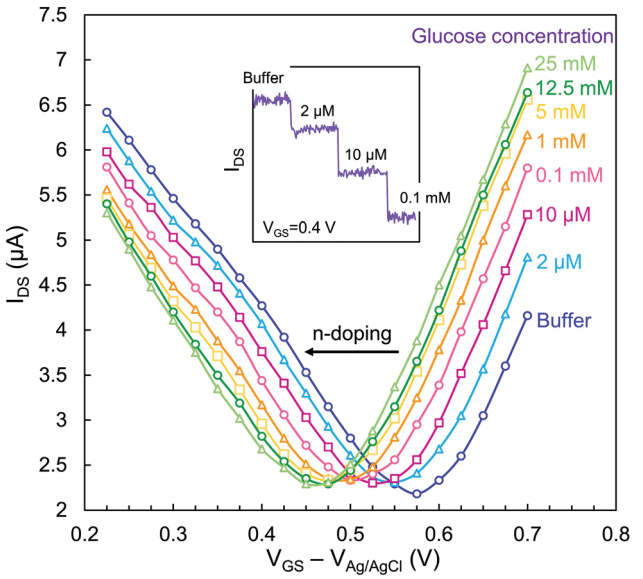


Fig. 3 Transfer characteristics measured when the device was exposed to glucose solutions (concentration ranging from 2 μM to 25 mM). The curve shifted to the left as a result of the increase in the glucose concentration. Inset: monotonic decrease of $I_{DS}$ at $V_{GS}$ = 0.4 V.

tested by exposure to glucose solution at different concentrations. The transfer characteristics curve was found to shift to the left significantly. For example, the shift was ~0.115 V as the glucose concentration increased from 0 to 25 mM (Fig. 3). This suggests that the binding of glucose and boronic acid generated n-type doping to graphene. As the estimated transconductance (*i.e.*, the slope of linear sections of the transfer characteristics curve) did not change significantly, the carrier mobility of the graphene were believed to be approximately constant (see details in ESI†). Rather, changes in the carrier concentration of graphene was considered the main contributor to the observed shift of $V_{NP}$. Measurements using butyric-acid functionalized graphene were also performed to serve as control (see details in ESI†). We also examined variations in the source–drain current $I_{DS}$ with the glucose concentration at a fixed gate voltage $V_{GS}$. It was observed that $I_{DS}$ decreased monotonically with glucose concentration when $V_{GS}$ was lower than the neutral point voltage $V_{NP}$, and this trend was reversed when $V_{GS} > V_{NP}$ (Fig. 3), which was due to the shift of the transfer characteristics. Using this observed dependence of $I_{DS}$ on the glucose concentration, we estimate that, with a noise level of ~17 nA for $I_{DS}$, the resolution of the nanosensor for glucose measurements was approximately 0.46 μM, appropriate for monitoring of glucose in human bodily fluids such as saliva and tears.[15,16]

We further studied the change of $V_{NP}$ before and after PBA functionalization, denoted $\Delta V_{NP,B}$, and the further changes of $V_{NP}$ after the graphene was exposed to glucose, denoted $\Delta V_{NP,G}$. Here, $\Delta V_{NP,B} = V_{NP,B} - V_{NP,P}$, and $\Delta V_{NP,G} = V_{NP,B} - V_{NP,G}$, where $V_{NP,P}$ and the $V_{NP,B}$ are the neutral point voltages measured in fresh buffer for pristine graphene and PBA-functionalized graphene, respectively; $V_{NP,G}$ is the neutral point voltage for PBA-functionalized graphene measured in glucose solution. We observed that both $\Delta V_{NP,B}$ and $\Delta V_{NP,G}$ varied from device to device, possibly because of artifacts such as organic residue left on graphene from the fabrication process. These artifacts could have caused a device-to-device disparity in chemical functionalization of graphene, and hence in the doping level at a given glucose concentration. Interestingly, at a given concentration, the ratio $\Delta V_{NP,G}/\Delta V_{NP,B}$ did not vary significantly from device to device, with a variation of less than 6% for the three nanosensor devices tested (Fig. 4). To explain this observation, we note that $\Delta V_{NP,B}$ is the shift of $V_{NP}$ caused by functionalization of boronic acid and $\Delta V_{NP,G}$ is by glucose-boronic acid binding, therefore $\Delta V_{NP,G}/\Delta V_{NP,B}$ can be regarded as a measure of the fraction of boronic acid that is occupied by glucose. Since under conditions of constant temperature and pH as were approximately the case in our experiment, the

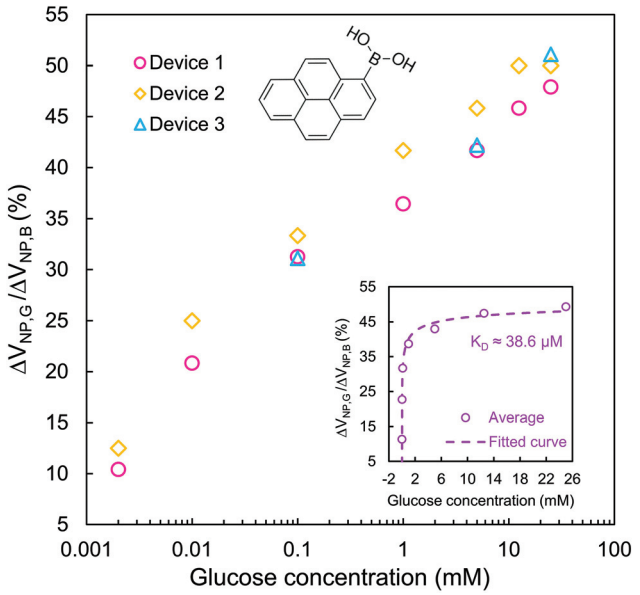


Fig. 4 Neutral point voltage shift ratio $\Delta V_{NP,G}/\Delta V_{NP,B}$ as a function of glucose concentration. Glucose concentration is on logarithmic scale. Inset: The solid line is a fit to the Hill–Langmuir equation, yielding an equilibrium dissociation constant ($K_D$) of 38.6 μM. Glucose concentration is on linear scale.

fraction of boronic acid that binds to glucose is solely dependent on the glucose concentration. This suggests that $\Delta V_{NP,G}/\Delta V_{NP,B}$ should be a function of glucose only and independent of the device or the order in which the sample solution was added. The measured dependence of this ratio on glucose concentration followed the Hill–Langmuir equation for equilibrium ligand-receptor binding (see details in ESI†); a least squares fit yielded an equilibrium dissociation constant ($K_D$) of 38.6 μM (Fig. 4), which is in agreement with a previous report and is appropriate for practical glucose sensing applications.[19]

While the exact mechanisms for the graphene affinity sensing remain open, some theoretical considerations can offer insight into the observed doping effects induced by chemical functionalization and glucose-boronic acid binding. First, to explain the observed p-type doping due to the attachment of PBA (Fig. 2a), we note that while pyrene group is electron-rich and not expected to induce p-doping, boronic acid is electron deficient and its electron-withdrawing nature could induce p-doping in the graphene. This is supported by our experiments in which immobilization of electron-rich groups on graphene (such as butyric acid, a carboxylic acid) resulted in n-type doping in the graphene (Fig. S4†), and also in agreement with experimental observations reported by others.[27,29] Second, the observed n-type doping due to the boronic acid-glucose binding was likely the result of an increase in the local electrostatic potential in the proximity of graphene, as suggested by results from a potentiometric study of glucose detection by boronic acid,[30,31] which resembles our graphene nanosensor in electrode configuration. This electrostatic potential increase could be attributed to the formation of boronate, which would increase the electron donating ability of boronic acid while weakening its electron-withdrawing ability.[31]

These conjectured sensing mechanisms suggest that immobilization of boronic acid on graphene or even other semiconducting materials, using other attachment groups should also allow for glucose recognition. Indeed, measurements of glucose using graphene that was modified with 9-anthraceneboronic acid (Fig. S5†) were found to be qualitatively consistent with results obtained with PBA as presented above. The corroboration of these mechanisms, however, requires a systematic study in future work. Further insight into the underlying physics may also lead to important improvements in the sensor performance. In particular, affinity sensors that use boronic acid (which forms boronate by binding to diol groups), including our current nanosensor (Fig. S6†), is in general not capable of distinguishing between different diol-containing monosaccharides. Although they may still be adequate for practical glucose detection in physiological fluids where glucose is present at dominant concentrations,[32,33] we anticipate that it is possible to chemically modify boronic acid-based receptors to impart glucose-specificity to the nanosensor over other monosaccharides,[34] which will also be a major subject of our future investigation.

## Conclusions

In conclusion, a graphene nanosensor is presented for affinity-based detection of low-charge, low-molecular-weight molecules, using glucose as a representative analyte. The nanosensor employed a graphene field-effector transistor in which graphene was functionalized with boronic acid for glucose recognition. The boronic acid was attached to graphene *via* the interaction between graphene and pyrene groups, allowing sensitive detection of electrically neutral glucose molecules. Testing results demonstrated that the nanosensor was capable of measuring glucose in a practically relevant range of 2 μM to 25 mM, with a resolution of 0.46 μM. The observed shifts of the transfer characteristics strongly suggested that recognition of glucose was due to the formation of glucose-boronate ester, which could reduce the boronic acid-induced p-type doping in the graphene. For practical clinical applications, it is expected that the nanosensor can be highly miniaturized without the use of mechanical moving parts or physical barriers, and hence be of practical utility in glucose monitoring.

## Acknowledgements

This work was supported by the National Institutes of Health (Grant No. 1DP3 DK101085-01), the National Science Foundation (Grant No. ECCS-1509760), and the National Natural Science Foundation of China (Grant No. 61428402). Y. Z. gratefully acknowledges a National Scholarship (Award No. 201206250034) from the China Scholarship Council. The

 

authors also appreciate helpful discussions with Xue Liu (Tulane University), Junyi Shang (Columbia University), Cheng Wang (Tsinghua University), and Jaeeun Yu (Columbia University). This study made use of the instrument in the cleanroom of Columbia University and of the Advanced Science Research Center at the City University of New York.

## Notes and references

1 J. H. An, S. J. Park, O. S. Kwon, J. Bae and J. Jang, *ACS Nano*, 2013, **7**, 10563–10571.
2 S. W. Zeng, K. V. Sreekanth, J. Z. Shang, T. Yu, C. K. Chen, F. Yin, D. Baillargeat, P. Coquet, H. P. Ho, A. V. Kabashin and K. T. Yong, *Adv. Mater.*, 2015, **27**, 6163–6169.
3 L. Gao, Q. Li, R. Li, L. Yan, Y. Zhou, K. Chen and H. Shi, *Nanoscale*, 2015, **7**, 10903–10907.
4 Y. B. Zhu, C. Wang, N. Petrone, J. Yu, C. Nuckolls, J. Hone and Q. Lin, *Appl. Phys. Lett.*, 2015, **106**, 123503.
5 F. Schedin, A. K. Geim, S. V. Morozov, E. W. Hill, P. Blake, M. I. Katsnelson and K. S. Novoselov, *Nat. Mater.*, 2007, **6**, 652–655.
6 C. Wang, J. Kim, Y. B. Zhu, J. Y. Yang, G. H. Lee, S. Lee, J. Yu, R. J. Pei, G. H. Liu, C. Nuckolls, J. Hone and Q. Lin, *Biosens. Bioelectron.*, 2015, **71**, 222–229.
7 Y. H. Kwak, D. S. Choi, Y. N. Kim, H. Kim, D. H. Yoon, S. S. Ahn, J. W. Yang, W. S. Yang and S. Seo, *Biosens. Bioelectron.*, 2012, **37**, 82–87.
8 M. Zhang, C. Z. Liao, C. H. Mak, P. You, C. L. Mak and F. Yan, *Sci. Rep.*, 2015, **5**, 8311.
9 S. Mansouri and J. S. Schultz, *Nat. Biotechnol.*, 1984, **2**, 885–890.
10 M. Lei, A. Baldi, E. Nuxoll, R. A. Siegel and B. Ziaie, *Diabetes Technol. Ther.*, 2006, **8**, 112–122.
11 X. Huang, C. Leduc, Y. Ravussin, S. Q. Li, E. Davis, B. Song, D. C. Li, K. X. Xu, D. Accili, Q. Wang, R. Leibel and Q. Lin, *Lab Chip*, 2014, **14**, 294–301.
12 Y. J. Heo, H. Shibata, T. Okitsu, T. Kawanishi and S. Takeuchi, *Proc. Natl. Acad. Sci. U. S. A.*, 2011, **108**, 13399–13403.
13 H. Shibata, Y. J. Heo, T. Okitsu, Y. Matsunaga, T. Kawanishi and S. Takeuchi, *Proc. Natl. Acad. Sci. U. S. A.*, 2010, **107**, 17894–17898.
14 R. Badugu, J. R. Lakowicz and C. D. Geddes, *Analyst*, 2004, **129**, 516–521.
15 Q. Y. Yan, B. Peng, G. Su, B. E. Cohan, T. C. Major and M. E. Meyerhoff, *Anal. Chem.*, 2011, **83**, 8341–8346.
16 C. Jurysta, N. Bulur, B. Oguzhan, I. Satman, T. M. Yilmaz, W. J. Malaisse and A. Sener, *J. Biomed. Biotechnol.*, 2009, **2009**, 430426.
17 D. K. Sen and G. S. Sarin, *Br. J. Ophthalmol.*, 1980, **64**, 693–695.
18 L. Zhang, Z. Y. Zhang, R. P. Liang, Y. H. Li and J. D. Qiu, *Anal. Chem.*, 2014, **86**, 4423–4430.
19 M. B. Lerner, N. Kybert, R. Mendoza, R. Villechenon, M. A. B. Lopez and A. T. C. Johnson, *Appl. Phys. Lett.*, 2013, **102**, 183113.
20 X. Huang, S. Q. Li, E. Davis, C. Leduc, Y. Ravussin, H. G. Cai, B. Song, D. C. Li, D. Accili, R. Leibel, Q. Wang and Q. Lin, *J. Micromech. Microeng.*, 2013, **23**, 055020.
21 G. Yoon, *Biosens. Bioelectron.*, 2011, **26**, 2347–2353.
22 X. S. Li, W. W. Cai, J. H. An, S. Kim, J. Nah, D. X. Yang, R. Piner, A. Velamakanni, I. Jung, E. Tutuc, S. K. Banerjee, L. Colombo and R. S. Ruoff, *Science*, 2009, **324**, 1312–1314.
23 Y. F. Hao, Y. Y. Wang, L. Wang, Z. H. Ni, Z. Q. Wang, R. Wang, C. K. Koo, Z. X. Shen and J. T. L. Thong, *Small*, 2010, **6**, 195–200.
24 J. W. Li, Y. Y. Liu, Y. Qian, L. Li, L. H. Xie, J. Z. Shang, T. Yu, M. D. Yi and W. Huang, *Phys. Chem. Chem. Phys.*, 2013, **15**, 12694–12701.
25 S. S. Li, Q. Zhou, W. Y. Chu, W. Zhao and J. W. Zheng, *Phys. Chem. Chem. Phys.*, 2015, **17**, 17638–17645.
26 K. Krishnan, *Proc. - Indian Acad. Sci., Sect. A*, 1963, **57**, 103–108.
27 X. C. Dong, D. L. Fu, W. J. Fang, Y. M. Shi, P. Chen and L. J. Li, *Small*, 2009, **5**, 1422–1426.
28 A. Das, S. Pisana, B. Chakraborty, S. Piscanec, S. K. Saha, U. V. Waghmare, K. S. Novoselov, H. R. Krishnamurthy, A. K. Geim, A. C. Ferrari and A. K. Sood, *Nat. Nanotechnol.*, 2008, **3**, 210–215.
29 D. B. Farmer, R. Golizadeh-Mojarad, V. Perebeinos, Y. M. Lin, G. S. Tulevski, J. C. Tsang and P. Avouris, *Nano Lett.*, 2009, **9**, 388–392.
30 H. Ciftci, U. Tamer, M. Sen Teker and N. O. Pekmez, *Electrochim. Acta*, 2013, **90**, 358–365.
31 E. Shoji and M. S. Freund, *J. Am. Chem. Soc.*, 2002, **124**, 12486–12493.
32 T. Kawasaki, H. Akanuma and T. Y. Yamanouchi, *Diabetes Care*, 2002, **25**, 353–357.
33 C. Sugnaux and H. A. Klok, *Macromol. Rapid Commun.*, 2014, **35**, 1402–1407.
34 X. Wu, Z. Li, X.-X. Chen, J. S. Fossey, T. D. James and Y.-B. Jiang, *Chem. Soc. Rev.*, 2013, **42**, 8032–8048.